

Real-time localization of sources using the phase and amplitude gradient estimator for acoustic intensity

Jacey G. Young, Joseph S. Lawrence, and Kent L. Gee

Citation: *Proc. Mtgs. Acoust.* **33**, 030001 (2018); doi: 10.1121/2.0000929

View online: <https://doi.org/10.1121/2.0000929>

View Table of Contents: <https://asa.scitation.org/toc/pma/33/1>

Published by the [Acoustical Society of America](#)

ARTICLES YOU MAY BE INTERESTED IN

[Design considerations for a Compact Correlation Velocity Log](#)

Proceedings of Meetings on Acoustics **33**, 070003 (2018); <https://doi.org/10.1121/2.0000928>

[A micro-mechanical model for the Biot theory of acoustic waves in a fully saturated granular material](#)

Proceedings of Meetings on Acoustics **35**, 005001 (2018); <https://doi.org/10.1121/2.0000936>

[New research on low-frequency membrane absorbers](#)

Proceedings of Meetings on Acoustics **33**, 015001 (2018); <https://doi.org/10.1121/2.0000816>

[Feasibility study of using acoustic methods for regionalizing an impact force acting on a structure](#)

Proceedings of Meetings on Acoustics **33**, 065002 (2018); <https://doi.org/10.1121/2.0000924>

[Acoustic field around a planar object levitated in an ultrasound waveguide](#)

Proceedings of Meetings on Acoustics **34**, 030005 (2018); <https://doi.org/10.1121/2.0000890>

[Proof of concept: Machine learning based filling level estimation for bulk solid silos](#)

Proceedings of Meetings on Acoustics **35**, 055002 (2018); <https://doi.org/10.1121/2.0000945>



175th Meeting of the Acoustical Society of America

Minneapolis, Minnesota

7-11 May 2018

Engineering Acoustics: Paper 3aEAb1

Real-time localization of sources using the phase and amplitude gradient estimator for acoustic intensity

Jacey G. Young

Department of Physics, Saint Norbert College, De Pere, WI, 54115; jacey.young@snc.edu

Joseph S. Lawrence and Kent L. Gee

Department of Physics and Astronomy, Brigham Young University, Provo, UT; joseph-lawrence@hotmail.com; kentgee@byu.edu

Recent demonstrations of real-time source localization systems have used a variety of direction-finding methods. One such system uses a multi-microphone probe to estimate acoustic intensity [Inoue et al., *Proc. Meetings Acoust.* 29, 025001 (2016)], although the bandwidth of intensity estimates are traditionally limited by the microphone spacing. The Phase and Amplitude Gradient Estimator (PAGE) method [Thomas et al., *J. Acoust. Soc. Am.* 137, 3366–3376 (2015)] greatly extends the bandwidth of active intensity, providing an accurate method of source localization for a wide bandwidth. An initial system implemented in LabVIEW estimates active intensity using the PAGE method to identify the direction of the source location in real time. Using a paired webcam, the program then overlays the direction as a three-dimensional arrow onto a webcam image. An experiment in an anechoic chamber shows the accuracy of the system is approximately five degrees within the camera's field of view and the application of real-time drone tracking is also discussed.



1. INTRODUCTION

Many methods of acoustic localization exist, with beamforming being one of the most prevalent. However, since beamforming requires a large array of microphones to be effective, it is not a convenient or low-expense method and presents several difficulties¹. An alternate method of localization using acoustic intensity has also been developed². This method uses fewer microphones, although the bandwidth of accurate intensity estimates is limited, determined by the microphone spacing. Despite the limited bandwidth, intensity-based localization has successfully utilized in a number of systems including a system developed by Inoue *et al.*³ using augmented reality, the Acoustic Compass⁴, and the SOUND CAM⁵.

To extend bandwidth in active intensity estimation, the Phase and Amplitude Gradient Estimator (PAGE) method has been developed.^{6,7} Similar to traditional intensity estimation, the method uses a multi-microphone probe. However, use of the phase gradient allows for accurate estimation up to the spatial Nyquist frequency, and beyond if the phase can be unwrapped.⁸ The method has been seen experimentally to extend bandwidth by at least an order of magnitude beyond that of traditional methods.⁹ A three-dimensional (3D) direction of arrival estimate can be obtained using a four-microphone probe. This paper presents a real-time localization system, utilizing PAGE active intensity to achieve direction of arrival estimation with extended bandwidth for a low microphone count. The system consists of LabVIEW software, using a web camera and a multi-microphone probe.

2. SYSTEMS OVERVIEW

For the real-time localization device, we created a system consisting of a spherical microphone probe, NI Data Acquisition unit, LabVIEW, and a simple web camera. The microphone probe is a G.R.A.S. 60LK spherical probe with four pre-polarized microphones arranged in a tetrahedral configuration. The probe has a diameter of 2.54 cm (1 inch), resulting in a spatial Nyquist frequency of 4400 Hz.¹⁰ Since the microphones are embedded into a sphere instead of being freely suspended, the distance between the microphones is multiplied by 3/2 for intensity calculations.¹¹ A National Instruments NI-9233 collects the data, which are sent to the LabVIEW software via USB 3.0. A web camera is also connected to the LabVIEW software. This allows for a live video feed, on which the direction of arrival is superimposed. The multi-microphone probe and the web camera are inserted into a 3D printed handle. As can be seen in Fig. 1, this allows the user to move them as a unit, aligning the coordinate systems of the camera and the calculated intensity vectors from the multi-microphone probe.



Figure 1. The 3D printed holder with the web camera and the spherical microphone probe.

3. SOFTWARE

Taking measurements from the multi-microphone probe, the LabVIEW software determines direction of arrival for a particular frequency, displaying it on a webcam image. Using NI Vision and NI Vision Assistant from LabVIEW's Sound and Vibration Toolkit and Vision Acquisition, the code works in three stages as laid out in more detail below. The code first calculates the sound intensity vector using data from the spherical probe. From here, it creates a three-dimensional arrow that is oriented according to the angles determined by the sound intensity vector. Finally, the code converts the three-dimensional arrow into a two-dimensional image which is superimposed onto a live camera feed.

A. INTENSITY CALCULATION

After LabVIEW collects the data from the multi-microphone probe, the acoustic vector intensity is calculated using the Pressure and Amplitude Gradient Estimator (PAGE) method in order to extend estimation bandwidth.⁶ In this method, the complex pressure is treated as a magnitude and phase, $p = Pe^{-j\phi}$, rather than using real and imaginary parts of the complex pressure. Particle velocity is determined using Euler's equation, $\mathbf{u} = (j/\rho_0\omega)\nabla p$, and active intensity is calculated by combining pressure and particle velocity, as $\mathbf{I} = \frac{1}{2}\text{Re}\{p\mathbf{u}^*\}$. The PAGE form of active intensity, expressed in terms of pressure amplitude and phase, is

$$\mathbf{I} = \frac{1}{\omega\rho_0}P^2\nabla\phi, \quad (1)$$

where ω is the angular frequency, ρ_0 is the air pressure, P is the center pressure magnitude, and $\nabla\phi$ is the phase gradient.

By using P and $\nabla\phi$ in Eq. (1), instead of the real and imaginary parts of the complex pressure, finite-sum and finite-difference errors in estimation of center pressure and particle velocity can be avoided.⁷ The PAGE method has been shown experimentally to accurately estimate the acoustic intensity up to the spatial Nyquist frequency, and with unwrapping being applied, past the spatial Nyquist for broadband sources.⁹ This project serves to validate use of PAGE intensity for direction-finding, showing that it can be accurate above the spatial Nyquist frequency.

This section of the code reads in the data passed through the Data Assistant Express VI into LabVIEW at a rate of 25,000 Hz and a block size of 10,000. For each microphone pair, a transfer function phase is calculated, which is unwrapped with an unwrapping function. The result is a phase matrix by microphone pair. From here, a pairwise phase difference of the data leads to a least-squares estimate of the phase gradient. When combined with the center pressure magnitude, estimated by averaging the pressure magnitudes at the microphones, the estimate for active intensity in Eq. (1) is obtained. This results in a three-dimensional intensity matrix with each column representing a different frequency and each row one of the three Cartesian dimensions.

B. ARROW GENERATION

The arrow generation section of code uses the intensities from the previous section to calculate the angles of arrival, and creates a three-dimensional arrow oriented in the specified direction. In order to do this, the program requires the user to choose a frequency range they would like to investigate. This is done in the frequency selection tab by either typing in a frequency with a range or moving a cursor over the desired frequency on the graph as shown in Fig. 2. Within the desired frequency range, the code selects the frequency with the maximum intensity. Then by using that frequency's intensity vectors, the direction of arrival is split into two angles, where the azimuthal angle is

$$\phi = \tan^{-1}\left(\frac{I_x}{I_z}\right), \quad (2)$$

and the elevation angle is

$$\theta = \tan^{-1}\left(\frac{I_y}{I_z}\right). \quad (3)$$

Here, I_x , I_y , and I_z are components of the vector active intensity, with x pointing horizontally with respect to the camera image, y pointing vertically, and z pointing into the screen. From here, the virtual arrow rotates to the direction of those angles. The arrow's color is set to represent the magnitude of the acoustic intensity.

As LabVIEW does not have a preset arrow shape in 2D or 3D, a custom arrow is created before data collection occurs by joining a cylinder and a cone. A sphere is added to show the pivot point around which the arrow rotates.

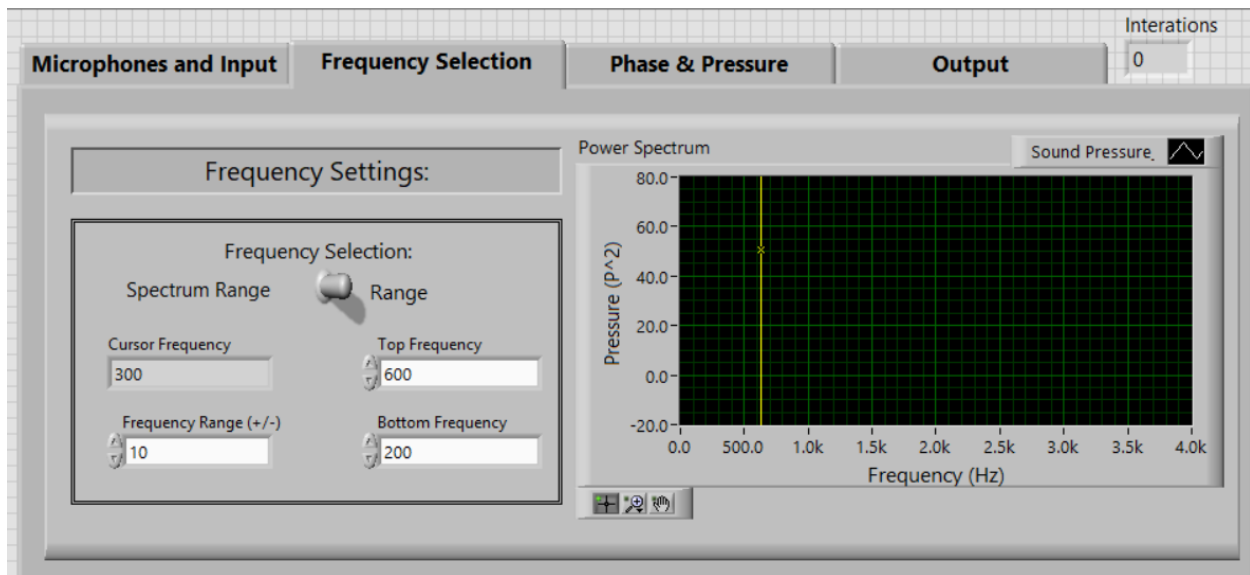


Figure 2. The frequency selection tab of the LabVIEW software. The user chooses a frequency range by either selecting a frequency with the graph cursor or by specifying a frequency range in the text boxes. The intensity with maximum magnitude in that range is used to estimate direction of arrival.

C. IMAGING OUTPUT

The final section of code takes the video feed image from the web camera and combines it with the three-dimensional arrow to produce the final output image. This section of code has two major parts, transitioning the three-dimensional arrow into a two-dimensional overlay, and the input and output of the web camera image. Both processes extensively use the NI Vision Assistant software.

The web camera input, processed in each iteration, take an image from the web camera and place it into the imaging code. Once in the imaging code, the image undergoes a series of overlays to position the arrow onto the image, as will be described further below. With the overlays completed, the image is sent to a IMAQ display for the user.

Transitioning the three-dimensional arrow to a two-dimensional overlay image was the biggest challenge of the imaging code. By setting up a series of overlays and masks, the arrow is first transitioned to a two-dimensional IMAQ image, with a cut out for the arrow on the web camera image and a second colored overlay image. An IMAQ Add VI is used to combine the web camera image and the two-dimensional overlay arrow. Smaller overlays are also used to make the final image more practical for the user. A yellow circle overlay was used to highlight the general area of the source on the camera image. If the source was outside the camera's field of view, no circle would appear and the arrow would simply point off the screen. Other overlays such as text outputs of the frequency of the sound source, the magnitude of the intensity, and the azimuthal and elevation angles for the direction of arrival, as defined in Eq. (2) and

Eq. (3), were also displayed on the image. A display of the output for a sound source off the screen can be seen on the right-hand side of Figure 3.

D. ADDITIONAL FEATURES

Other features were added to this code for more practical use. Such functions were running histories of decibel level and position of the sound source on the camera viewing screen, a noise threshold feature, a distance calibration feature, and a save data feature.

The distance calibration feature took into consideration the discrepancy between the vertical axis of the microphone probe and the camera while in the holder. This discrepancy, within certain limits, would affect the accuracy of the elevation angle and the yellow circle overlay. With the distance calibration, the corrected elevation angle is

$$\theta = \tan^{-1} \left(\frac{I_y}{I_z} - \frac{a}{d} \right) \quad (4)$$

where d is the distance in the z -direction between the microphone probe and the source and a is the vertical distance between the microphone probe and the camera. With this feature turned off, it was assumed that the microphone probe and camera coordinate systems were equal, which is approximately true for distances $d > 1\text{m}$.

The save data feature saved the elevation and azimuthal angles with their standard deviations, as well as the magnitude of the intensity and the frequency at which the software was analyzing at the time the data was saved.

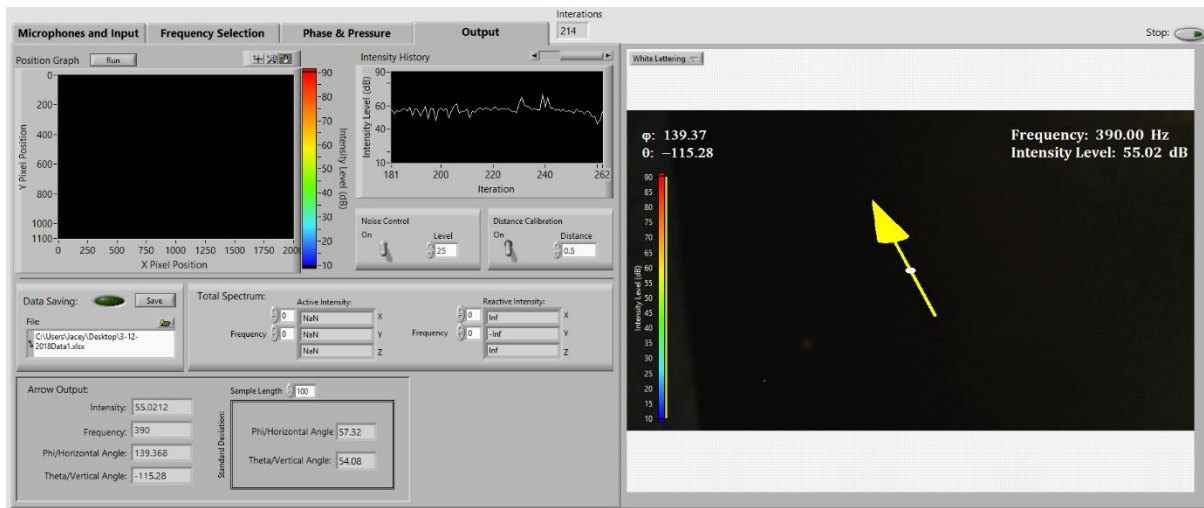


Figure 3. The output tab of the LabVIEW software (left) and the web camera image (right). Extra features such as running histories, the saving feature, noise threshold and a distance calibration can be found to the left side in the Output tab. The right side of the screen shows the image output (currently blank) with the arrow and text overlays.

4. EXPERIMENT

In order to test precision and accuracy of the angle of arrival as measured by our device, we set up an experiment with a white noise sound source and a scanning grid in an anechoic chamber. With this data, we were able to compare the azimuthal and elevation angles read from the software with the angles expected from the geometry to determine the standard deviations of the device's angles (precision), as well as the average angle error (accuracy). The azimuthal angle is the angle left or right from the vertical center axis

of the web camera image, while the elevation angle is the angle up or down from the horizontal center axis. Without distance calibration on, this elevation angle is assumed to be from approximately the same for both the camera and the microphone coordinate systems.

A. SETUP

We positioned the probe holder on a three-dimensional scanning system, 0.86 meters above a speaker playing white noise as shown in Fig. 4. From here, we moved the scanning system in a two-dimensional 11 by 11 grid with a spacing of 0.15 meters between each position. At each position we let the system come to rest and proceeded to take three data points through the save data feature within the application. The three data points represent three different frequencies within the white noise, 500 Hz, 2500 Hz, and 6000 Hz. The frequencies were selected using the frequency graph selection option within the program with a ± 15 Hz range around the designated frequency.



Figure 4. Experimental setup for determining the precision and accuracy of the azimuthal and elevation angles consisting of a white noise sound source (speaker) and the 3D handle unit attached to a 3D scanning system in the anechoic chamber.

B. RESULTS

The experiment showed angle error in degrees for both the azimuthal and elevation angle, which is plotted in Fig. 5. Angle error was determined by relating the angles received through the software to the angles calculated through the known distances from the speaker to the probe at each position. A correction for probe tilt was performed. Results over the entire scan show an average error of about 10 degrees for both angles at low frequencies. However, the error is much less in the field of view of the camera, which is about 5 degrees on average. Thus, the device appears to have a 5-degree uncertainty within the camera's view, and a larger error out of the camera's view. Furthermore, more errors appeared to be present as the frequency increased. This can most prominently be seen in the 6000 Hz, however, much of this error is likely due to scattering of the scanning system.

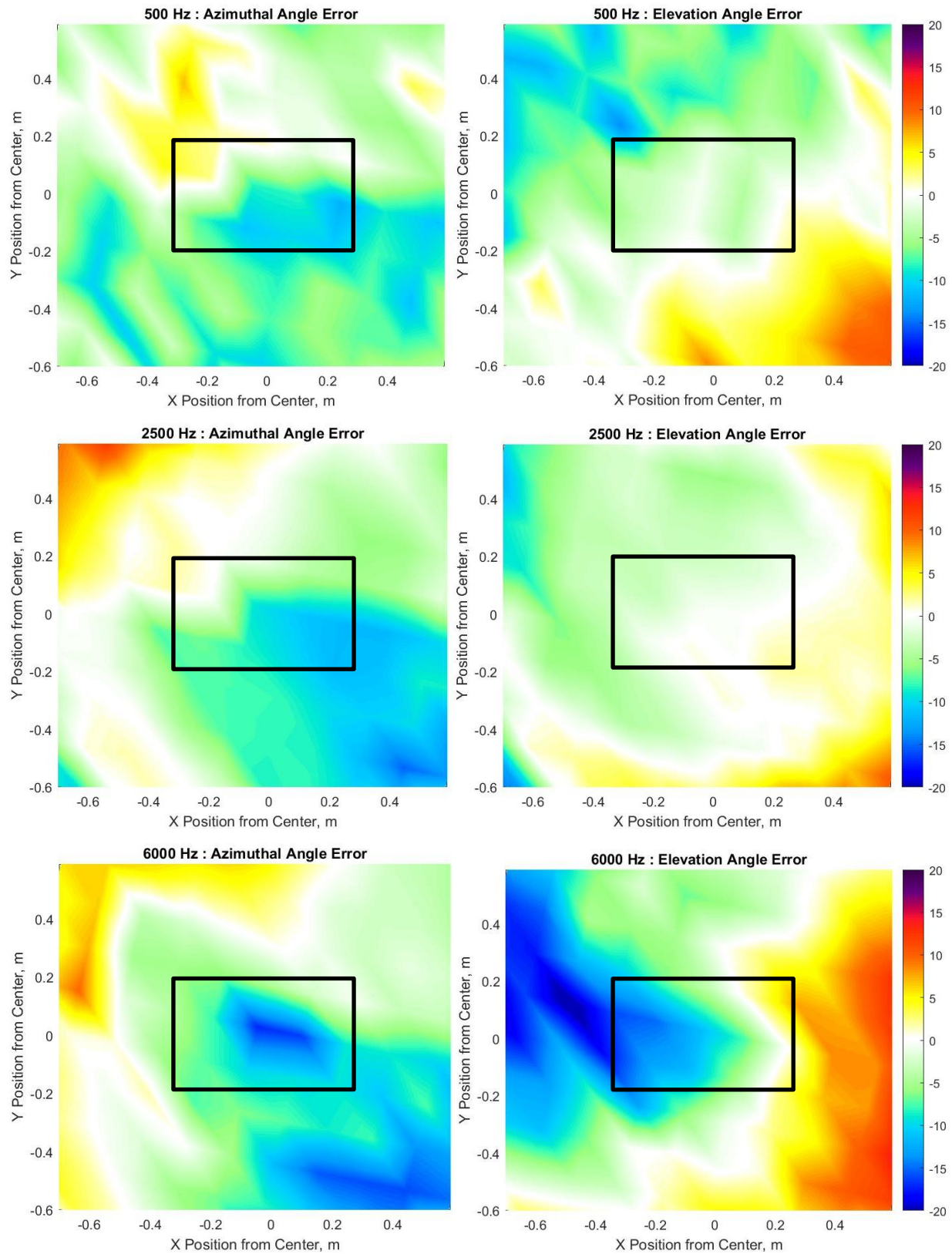


Figure 5. Experimental accuracy of the device for azimuthal and elevation angles, for 500, 2500 and 6000 Hz. The color represents the angle error in degrees and the position on the 2D plot represents the position in the scanning grid. The box represents the area in which the sound source is within the view of the camera.

C. DRONE TRACKING

To test the device in application, we tested tracking objects in real-time. Successful tracking of a quadcopter drone was performed in an anechoic chamber, a screenshot of which is shown in Fig. 6. An observed limitation of the device was the limited refresh rate, making it difficult to keep up with quickly-moving objects. However, within the refresh rate of the device, successful tracking was achieved.

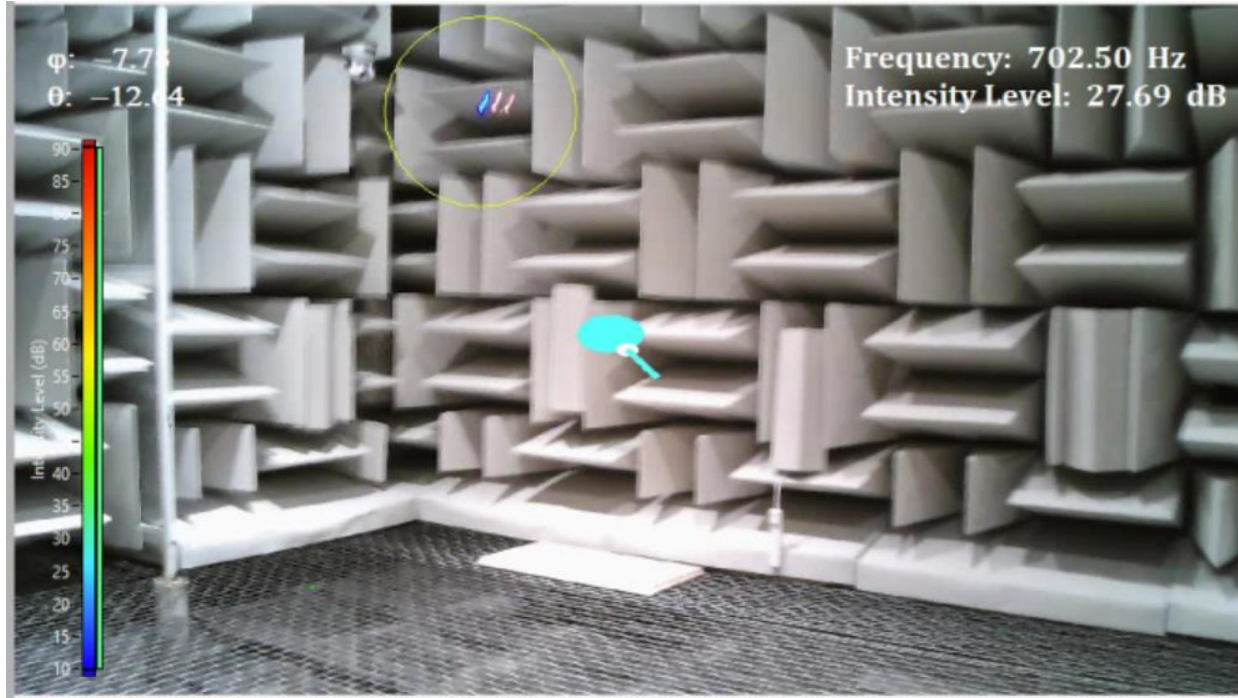


Figure 6. A screenshot of the software tracking a drone inside the anechoic chamber. The yellow circle overlay can be seen here identifying the area on the image where the sound source is coming from.

5. CONCLUSION

Through LabVIEW software, a real-time localization system was created using a handheld web camera, a multi-microphone probe, and a USB DAQ. The direction of arrival is estimated using active intensity, which allows for localization using a small number of microphones, and by utilizing the PAGE method the estimate has much greater bandwidth than in traditional estimation. The localization system was found to be accurate to within about five degrees in the camera's view. It was also seen to accurately track a drone within the frame rate of the camera in a controlled environment. Future work on this system may include visual improvements, improving framerate, and testing in less ideal acoustic environments. This software could also be adapted to other sound quantities, such as directional pressure.

ACKNOWLEDGMENTS

This research was funded by the National Science Foundation as part of the Research Experience for Undergraduates Program.

REFERENCES

- ¹ H. Ding, H. Lu, C. Li, J. Jing, D. Mei, and G. Chai. "Localization and identification of three-dimensional sound source with beamforming based acoustic tomography," Proc. Mtgs. Acoust. **19**, 065063 (2013).

- ² J. Y. Chung, "Cross-spectral method of measuring acoustic intensity without error caused by instrument phase mismatch," *J. Acoust. Soc. Am.* **64**, 1613–1616 (1978).
- ³ A. Inoue, Y. Ikeda, K. Yatabe, and Y. Oikawa. "Three-dimensional sound-field visualization system using head mounted display and stereo camera," *Proc. Mtgs. Acoust.* **29**, 025001 (2017).
- ⁴ <https://www.cae-systems.de/en/products/intensity-mapping/acoustic-compass.html>
- ⁵ <https://www.cae-systems.de/en/products/acoustic-camera-sound-source-localization/soundcam.html>
- ⁶ D. C. Thomas, B. Y. Christensen, and K. L. Gee, "Phase and amplitude gradient method for the estimation of acoustic vector quantities." *J. Acoust. Soc. Am.* **137**, 3366–3376 (2015)
- ⁷ E. B. Whiting, J. S. Lawrence, K. L. Gee, T. B. Neilsen, and S. D. Sommerfeldt, "Bias error analysis for phase and amplitude gradient estimation of acoustic intensity and specific acoustic impedance," *J. Acoust. Soc. Am.* **142**, 2208–2218 (2017).
- ⁸ M. R. Cook, K. L. Gee, S. D. Sommerfeldt, and T. B. Neilsen "Coherence-based phase unwrapping for broadband acoustic signals" *Proc. Mtgs. Acoust.* **30**, 055005 (2017).
- ⁹ K. L. Gee, T. B. Neilsen, S. D. Sommerfeldt, M. Akamine, and K. Okamoto, "Experimental validation of acoustic intensity bandwidth extension by phase unwrapping," *J. Acoust. Soc. Am.* **141**, EL357–EL362 (2017).
- ¹⁰ M. T. Rose, R. D. Rasband, K. L. Gee, and S. D. Sommerfeldt, "Comparison of multi-microphone probes and estimation methods for pressure-based acoustic intensity." *Proc. Mtgs. Acoust.* **26**, 030004 (2016).
- ¹¹ C. P. Wiederhold, K. L. Gee, J. D. Blotter, S. D. Sommerfeldt, and J. H. Giraud, "Comparison of multimicrophone probe design and processing methods in measuring acoustic intensity," *J. Acoust. Soc. Am.* **135**, 2797–2807 (2014).